Capability of the PAMELA Time-Of-Flight to identify light nuclei: results from a beam test calibration

D. Campana [a], R. Carbone [a,d], G. De Rosa [b], G. Osteria [a,*], S. Russo [b], W. Menn [c], V. Malvezzi [d], L. Marcelli [d], P. Picozza [d], R. Sparvoli [d], L. Bonechi [e], M. Bongi [f], S. Ricciarini [f], E. Vannuccini [f]

[a] *INFN, Section of Naples, Naples (Italy)*

[b] *Dept. of Physics, University of Naples and INFN, Naples (Italy)*

[c] *Dept. of Physics, University of Siegen, Siegen (Germany)*

[d] *Dept. of Physics, University of Rome Tor Vergata and INFN, Rome (Italy)*

[e] *Dept. of Physics, University of Florence and INFN, Florence (Italy)*

[f] *INFN, Section of Florence, Florence (Italy)*

Abstract

PAMELA is a space telescope orbiting around the Earth since June 2006. The scientific objectives addressed by the mission are the measurement of the antiprotons and positrons spectra in cosmic rays, the hunt for anti-nuclei as well as the determination of light nuclei fluxes from Hydrogen to Oxygen in a wide energy range and with very high statistics. In this paper the charge discrimination capabilities of the PAMELA Time-Of-Flight system for light nuclei, determined during a beam test calibration, will be presented.

Key words: Scintillation detectors, Cosmic rays, Abundances, Satellite-borne experiment
PACS: 29.40.Mc, 96.50.S-, 96.50.sb, 95.40.+s

* Corresponding authour: Address: Complesso Universitario di Monte S.Angelo Via Cintia 80126 Naples - ITALY; Phone: +39 081 676167; E-mail: giuseppe.osteria@na.infn.it

1 Introduction

The PAMELA apparatus is designed to study charged particles in the cosmic radiation. It is hosted by a Russian Earth-observation satellite, the Resurs-DK1, that was launched into space by a Soyuz rocket on the 15^{th} June 2006 from the Baikonur cosmodrome (Kazakhstan). The satellite orbit is elliptical and semi-polar, with an inclination of 70.0° and an altitude varying between 350 km and 600 km. The mission will last nominally for three years. The main scientific goal of the experiment is the precise measurement of the cosmic-ray antiproton and positron energy spectra. The satellite orbit and the mechanical design of the apparatus allow the identification of these particles in an unprecedented energy range (between 50 MeV and 270 GeV for positrons and between 80 MeV and 190 GeV for antiprotons) and with high statistics ($\sim 10^4$ antiprotons and $\sim 10^5$ positrons per year). Additionally PAMELA is searching for antimatter in the cosmic radiation, with a sensitivity for the anti-He/He ratio of the order of $\sim 10^{-7}$.

PAMELA is also aimed to extensively study the abundances and composition of light cosmic rays (up to Oxygen) over almost three decades of energy. In order to clarify the role of the different mechanisms that act in the propagation and transport of galactic cosmic rays it is fundamental to have more precise and extended data on the relative abundances of the constituents of galactic cosmic rays and especially on the ratio of secondary to primary particles, such as the Boron/Carbon ratio.

This paper will illustrate the light-charge identification capabilities of the PAMELA Time-Of-Flight (TOF) system, as evaluated during a beam test performed at the GSI laboratory - Germany - in February 2006. The TOF system is a key detector for the PAMELA instrument, providing trigger for acquisition, measuring the particle flight time (necessary to reject the albedo background component) and determining the absolute value of the particle charge. The paper is organized as follows: after an overview of the PAMELA instrument (section 2), the GSI beam test (set-up of the detector, available beams, operational details) is described in section 3. Section 4 is dedicated to the determination of the TOF time resolution from the beam data, obtained with two different methods, and finally section 5 reports the charge resolution of PAMELA TOF system for several elements, ranging from Proton to Carbon.

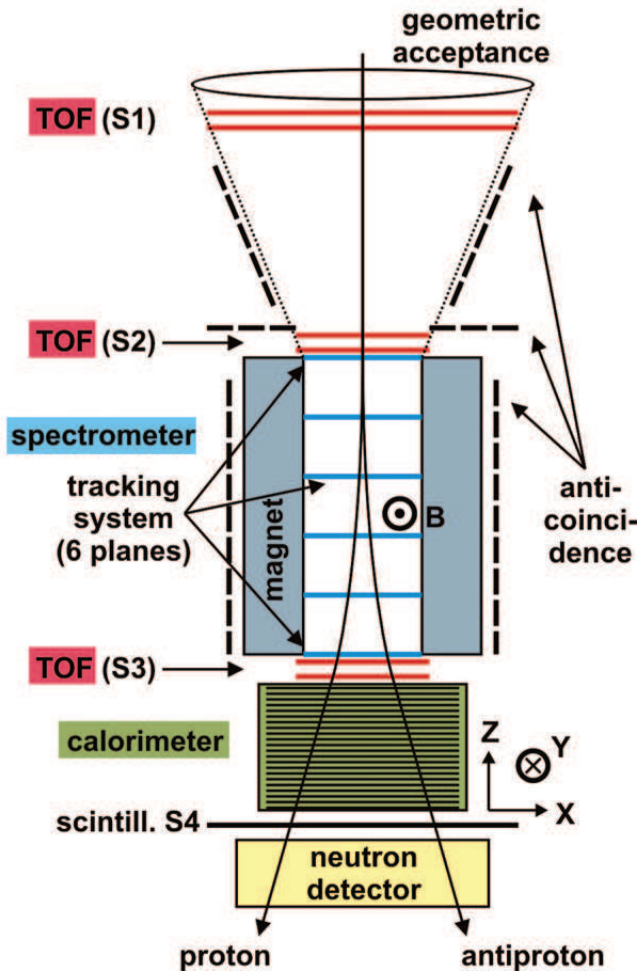

Fig. 1. A sketch of the PAMELA telescope. The method of discrimination between particle and antiparticle with the magnetic spectrometer is illustrated. The main direction of the magnetic field B inside the spectrometer is also shown.

2 The PAMELA instrument and the Time-Of-Flight system

The PAMELA apparatus, shown in Figure 1, is composed by several sub-detectors: TOF system, anticoincidence system, magnetic spectrometer with microstrip silicon tracking system, W/Si electromagnetic imaging calorimeter, shower-tail-catcher scintillator (S4) and neutron detector. A detailed description of the PAMELA instrument and an overview of the mission can be found in [1].

The instrument has maximum diameter of 102 cm and height of 120 cm; its mass is 470 kg, the maximum power consumption is 355 W. The magnetic spectrometer determines the charge sign and momentum of the incoming particle through the trajectory reconstruction in the magnetic field; downward-going particles are identified with the time-of-flight measurement operated by TOF.

The final identification (i.e. antiprotons against electrons etc.) is provided by the combination of the calorimeter and neutron detector information for kinetic energies above 1 GeV and by the velocity measurement (obtained from the trajectory and time-of-flight) at lower energies.
In what follows a synthetic description of the TOF system will be given; further details on the TOF detectors and electronics can be found in references [2] and [3] respectively.
The TOF system is composed of 6 layers of segmented plastic scintillators, arranged in three double planes (S1, S2, S3 in Figure 1). The distance between S1 and S2 is around 30 cm, while the S1-S3 distance is around 77 cm. Each layer is divided into several identical paddles (strips), whose number and dimensions vary from layer to layer, for a total of 24 paddles. For each double plane, the paddles of the upper layer are orthogonal to those of the lower layer, therefore allowing to get a bidimensional geometrical measurement of the impact point of charged particles. The plastic scintillator material, BC-404, manufactured by Bicron company, is characterized by a rise time of 700 ps and decay time of 1.8 ns. Both ends of each scintillator paddle are glued to an adiabatic UV-transmitting plexiglas light guide. The gluing is obtained with an optical cement, mod. BC-600 manufactured by Bicron. Each paddle is readout at each of its two ends by a photomultiplier tube (PMT) mod. R5900 by Hamamatsu Photonics. The R5900 is a 10-stage metal package head-on PMT, with rise time of 1.5 ns, achieving an amplification of about 4×10^6 at 900 V. It has a square section of $25.7 \times 25.7\,\mathrm{mm}^2$ and was chosen for its mechanical robustness, limited size and small weight (25.5 g). Since the core of the PAMELA apparatus is a permanent magnet, the PMTs have been shielded from the residual magnetic field of the spectrometer with a 1 mm thick μ-metal screen [2].
The anode pulse of each PMT is converted both in charge (ADC) and time (TDC). The ADC measurements can be used to determine the Z of the incoming particle. The combined TDC information of the whole TOF is used to generate the main PAMELA trigger and to measure the flight time of the incoming particle. The geometry of the TOF planes has been chosen to match the geometric acceptance of the spectrometer. The standard trigger configuration requires the coincidence of at least one TDC signal from each of the three TOF double planes.

3 GSI beam test

During its construction phase, PAMELA was tested three times with beams of protons and electrons at the CERN SPS accelerator, to study the performance of the subdetectors with relativistic particles. Because of the tight schedule of PAMELA integration, however, it was not possible to perform a beam test of

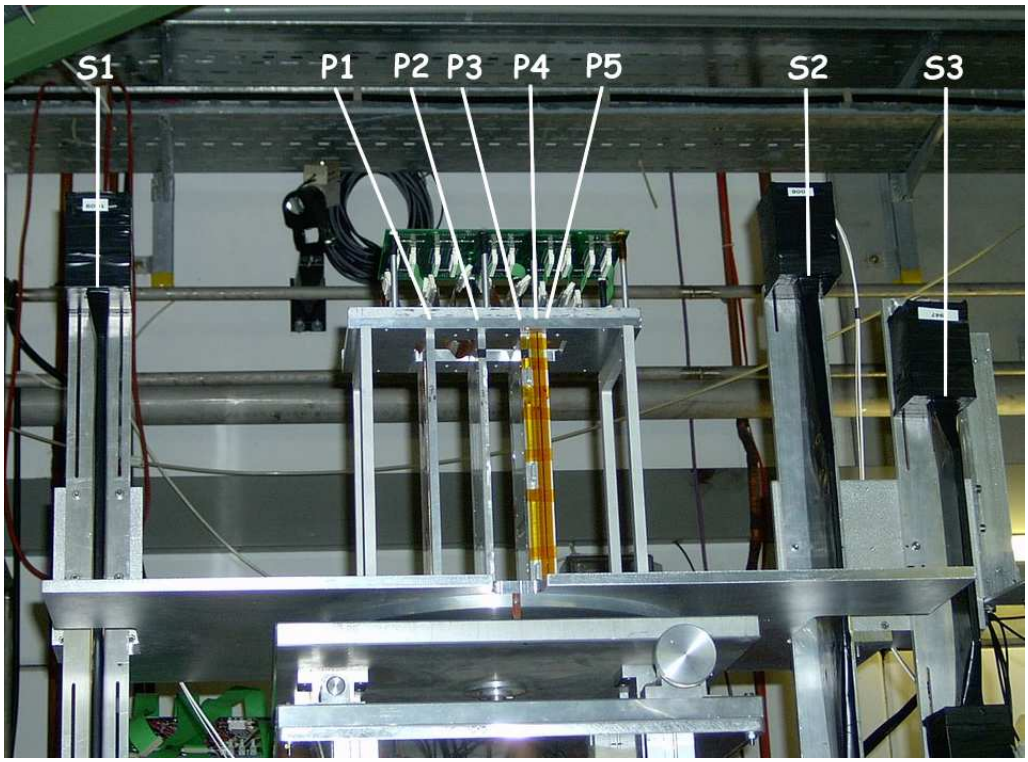

Fig. 2. The experimental set-up of PAMELA prototype at the GSI beam test. S1, S2 and S3 are the TOF system scintillators, while P1÷P5 are the silicon modules of the tracking system.

the flight model with light nuclei before its delivery to Russia in March 2005. For this reason such a light-nuclei test was performed by using prototypes of the PAMELA TOF and tracking system in a dedicated mechanical arrangement, on February 2006 at the GSI (Gesellschaft f*ü*r Schwerionenforschung, Darmstadt, Germany) beam accelerator. Figure 2 shows the arrangement of the instrument under test: in this set-up each TOF plane is formed by just one paddle (indicated as S1, S2, S3 in the picture), while the prototype of tracking system is composed by 5 Si detector modules (P1 to P5).

The main aim of the test was the determination of the time resolution of the TOF system and of the charge resolution both for the TOF and for the tracking system for light nuclei. In particular, the behaviour of these detectors was studied, to determine the amount of variation from linearity of the corresponding read-out electronics with energy releases due to $Z > 1$ particles. The test results on TOF performance will be presented in the next sections; results for tracking system will not be discussed here as they will be published elsewhere.
Data were taken during four full days. PAMELA was the secondary beam user for part of this time (during nights); when main user, it was possible to choose the best available value for beam intensity (around 1000 particles/spill, with a 4 s spill duration and a 3 s interval between subsequent spills); other-

wise, the intensity was much higher (up to 10^8 particles/spill) thus resulting in high trigger rate but also in a large fraction of multi-particle events in the detectors. For some runs, polyethylene or aluminium targets were employed to produce secondaries; besides, during night hours the presence of biological test-tubes of the main beam user, upstream the PAMELA prototype, acted as a target. The instrument was normally placed along the beam line, one meter beyond the target position. For some acquisitions the instrument was moved to a different position, at the same distance but along a 45° radial line from the target with respect to the beam line, to record only secondaries scattered at this high angle; these particles were mostly low-energy protons and He nuclei. Table 1 summarizes the different configurations used for the test. Three primary beams were available: ^{12}C with kinetic energy of 1200 MeV/n, ^{12}C with 200 MeV/n, ^{50}Cr with 500 MeV/n.

The TOF paddles used at GSI are identical to the ones of the corresponding flight-model layer; the dimensions of the paddles selected for the GSI test are: $(40.8 \times 5.5 \times 0.7)\,\mathrm{cm}^3$ for S1, $(18.0 \times 7.5 \times 0.5)\,\mathrm{cm}^3$ for S2 and $(18.0 \times 5.0 \times 0.7)\,\mathrm{cm}^3$ for S3. The three paddles were arranged with their main (longitudinal) dimension along the vertical axis. The S1-S3 distance at GSI was around 80 cm [4], while the S1-S2 distance was around 67 cm, greater than in the flight model. For this beam test the high voltages of the PMTs have been chosen in such a way to obtain a gain of 1×10^6 which, according to our calibrations, correspond to HV values varying from 780 V to 820 V.

As in the flight model, each paddle is read-out by two PMTs, thus giving a total of six ADC and six TDC signals. The trigger configuration requires the coincidence of at least one TDC signal from S1 and S2 paddles. The read-out electronics employed in this test is the same as for the flight model [3]. Concerning the prototype of tracking system used for the test, each detector module and its corresponding read-out electronics are identical to the ones employed in the flight model [5] [6]. To simplify the whole structure five silicon detector modules have been assembled in a simple aluminum frame in such a way to keep them aligned. The double-sided silicon sensors $(5.33 \times 7.00)\,\mathrm{cm}^2$ provide two independent impact coordinates on each plane. The high-resistivity n-type Si bulk is segmented with 1024 read-out microstrips for each side: p+ strips on the junction side (implantation pitch 25.5 μm, read-out pitch 51 μm) and n+ strips on the ohmic side (implantation and read-out pitch 66.5 μm). Junction-side (X-view) strips are orthogonal to ohmic-side (Y-view) ones.

4 TOF time resolution and β measurements

Two different methods have been used here to measure the time resolution of the TOF system. The first one combines information from the timing mea-

Table 1
BEAMS AVAILABLE AT THE GSI TEST

Particle	**Energy (MeV/n)**	**Target**	**Angle (deg.)**	**Events**
^{12}C	1200		0	269896
^{12}C	1200	×	0	123194
^{12}C	200		45	30378
^{12}C	200	×	45	196139
^{50}Cr	500		0	15976
^{50}Cr	500	×	0	173960
^{50}Cr	500	×	45	52241

surements of the TDCs and the position measurement of the tracking system; with this method it is possible to get the intrinsic time resolution of a TOF paddle. The second approach takes into account only the measurements of the TOF itself using the measurements of two paddles, as a result one will get the time resolution of the full TOF system.

In the first method we determine the intrinsic time resolution of a single paddle by taking information from both TOF and tracker. The position of the hit point along the scintillator x is proportional to the difference of the time measurements t_1 and t_2 at the two sides of the scintillator itself:

$$x = \frac{v_{eff}(t_1 - t_2)}{2} + K \tag{1}$$

where v_{eff} is the signal velocity inside the scintillator.

If the position of the incident particle along the paddle as determined from the timing of the pulses in the two PMTs (in units of picoseconds) is plotted versus the position as determined by the tracker, we obtain the scatter plot shown in figure 3.

A linear fit to the distribution is shown as well. This fit is used to derive the residuals for each event, thus getting finally the distribution of timing deviations from the tracker-position which is shown in figure 4.

Assuming negligible uncertainty in the projected position, the width of a Gaussian fitted to this distribution can be taken as the intrinsic time resolution of the paddle Δt_{Si}.

In this way it is possible to evaluate the time resolution of the single paddle of the TOF system for each family of nuclei (produced by fragmentation) from Hydrogen to Carbon, as summarized in table 2. As expected, we see

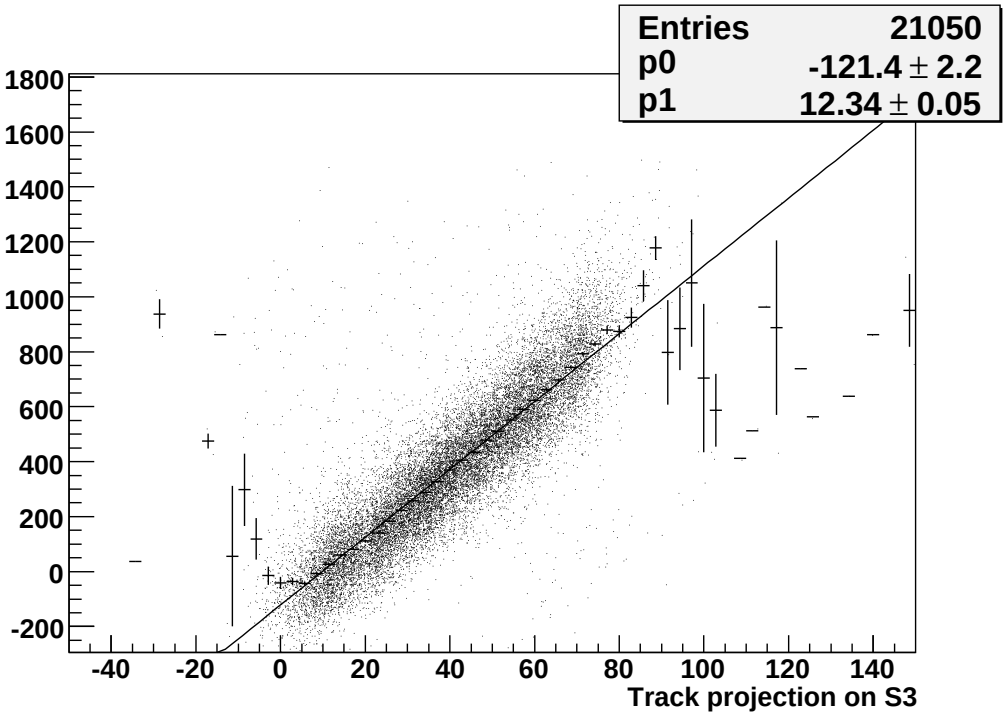

Fig. 3. Scatter plot of the crossing coordinate along paddle S3 as reconstructed through TDC measurement (in units of ps) versus the position measured by the tracking system (in mm). The linear fit and the corresponding bin measurements are superposed. The fit parameter p1 represents v_eff in cm/ns. The points with large error bars are due to poor statistics (regions of the paddle reached only by few particles).

an improvement in the time resolution for higher charges, since such particles produce more photons in the scintillator as for a proton of equal MeV/nucleon (according to the Bethe-Bloch equation the energy release and therefore the number of photons created in the scintillator increases with the square of the charge Z of the particle).

For ions of small Z it is necessary to take into account the *Time-Walk effect* [7]. In order to evaluate the dependence of the time resolution from the amplitude of the signal, the quantity to be considered is, for each PMT of a given paddle, the residual of each event from a linear fit analogous to that shown in figure 3 for the S3 paddle, versus the amplitude of the signal of the same PMT. The points in the resulting plots show a trend which is well fitted (see figure 5) by a typical function [8]:

$$t_{ij} = TDC_{ij} - (p_0 + \frac{p_1}{\sqrt{ADC_{ij}}} + \frac{p_2}{ADC_{ij}}) \quad , \tag{2}$$

where i (=1,2) is the PMT index and j (=1,2,3) is the scintillator paddle index.

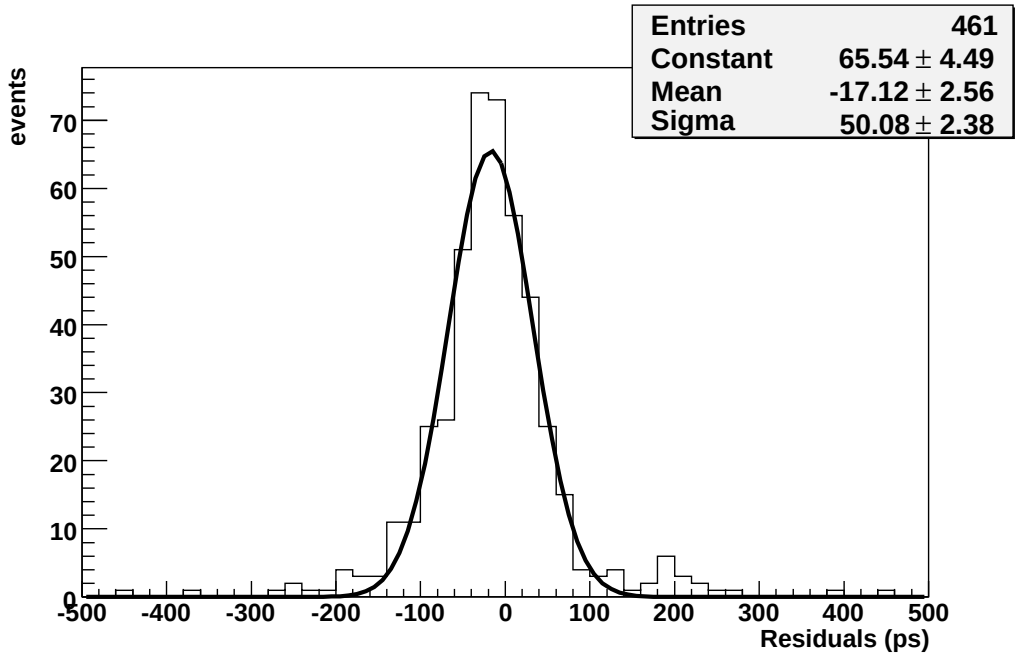

Fig. 4. Residual distribution for Boron sample in the S3 paddle; the standard deviation of this distribution is the intrinsic time resolution of this layer in *ps*.

Table 2
TIME RESOLUTION OF S3 PADDLE FOR DIFFERENT SAMPLES OF NUCLEI

Z	Δt **(ps)**	Δt **after Time-Walk correction(ps)**
1	146.5±0.9	117.3±0.7
2	131±5	122±4
3	118±4	114±4
5	50±2	50±2
6	46.5±0.3	46.5±0.3

By operating this time-amplitude correction we improved the time resolution up to Lithium (see last column of table 2).

To get the time resolution of the TOF with the second method we use two TOF paddles to derive the actual velocity β for a particle. Using the two paddles A and B we get four TDC measurements, t_1 and t_2 from paddle A, t_3 and t_4 from paddle B. While the difference of two measurements from a paddle is proportional to the position of the particle in the paddle (see equation 1), the sum of the two measurements can be taken as the "mean time" [9]. Thus the difference of the two sums will be proportional to the particle velocity between the two counters. If we define the "difference of

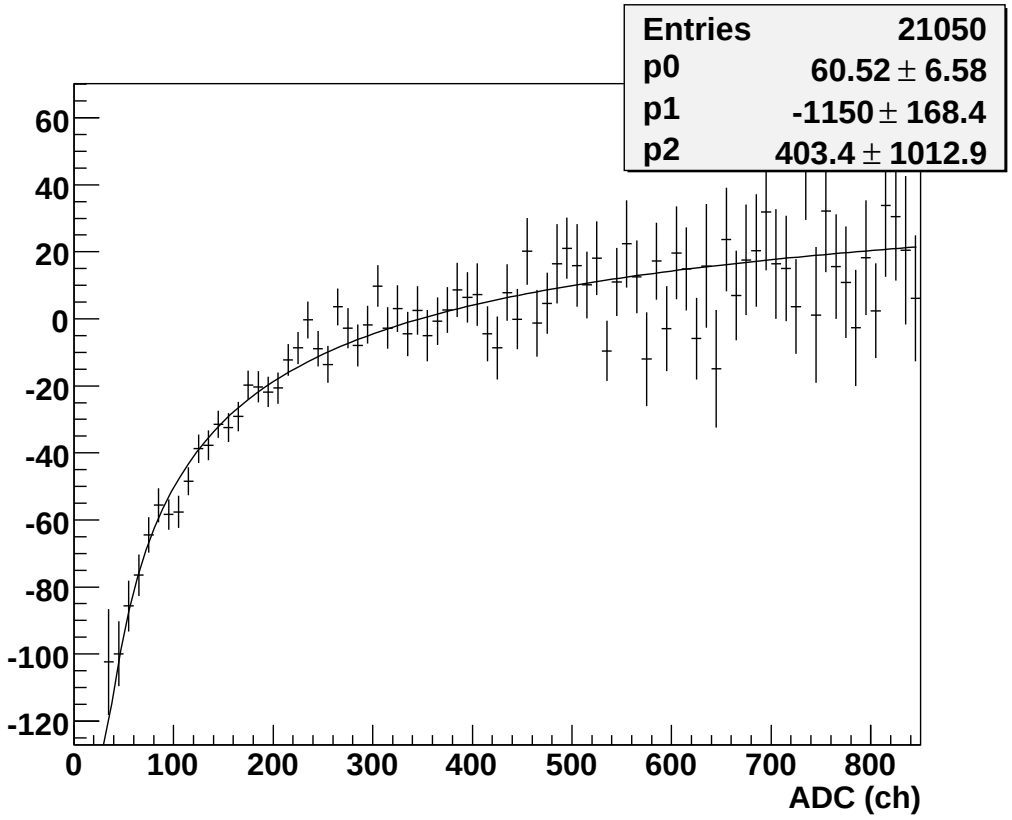

Fig. 5. Differences between the position of the hit point along the paddle S3 as reconstructed by the TOF alone with respect to the same position reconstructed by the tracking system, plotted versus the amplitude (in units of ADC channels) of the signal of one of the two PMTs of the paddle.

sums" DS as $DS = (t_1 + t_2) - (t_3 + t_4)$, we derive a simple equation between DS and the velocity β of the particle [10]:

$$DS = K_1 + K_2 \frac{1}{\beta cos\theta} \quad , \tag{3}$$

where K_1 and K_2 are two parameters which depend on the experimental setup, θ is the zenith angle. K_2 depends solely on known values: $K_2 = \frac{2L}{c}$, where L is the distance between the scintillator paddles and c is the speed of light. K_1 must be derived from the data itself, since it depends on unknown features of the experimental setup like cable lengths. To evaluate K_1 we measure DS for particles of known β and invert the equation 3. For this purpose we use, for each of the three types of beam, only data acquired with direct exposition of the apparatus to the beam (without polyethylene or aluminum target). The obtained values of K_1 for each couple of scintillators are consistent.

With the calculated values of the K_1 and K_2 constants we can reconstruct β.

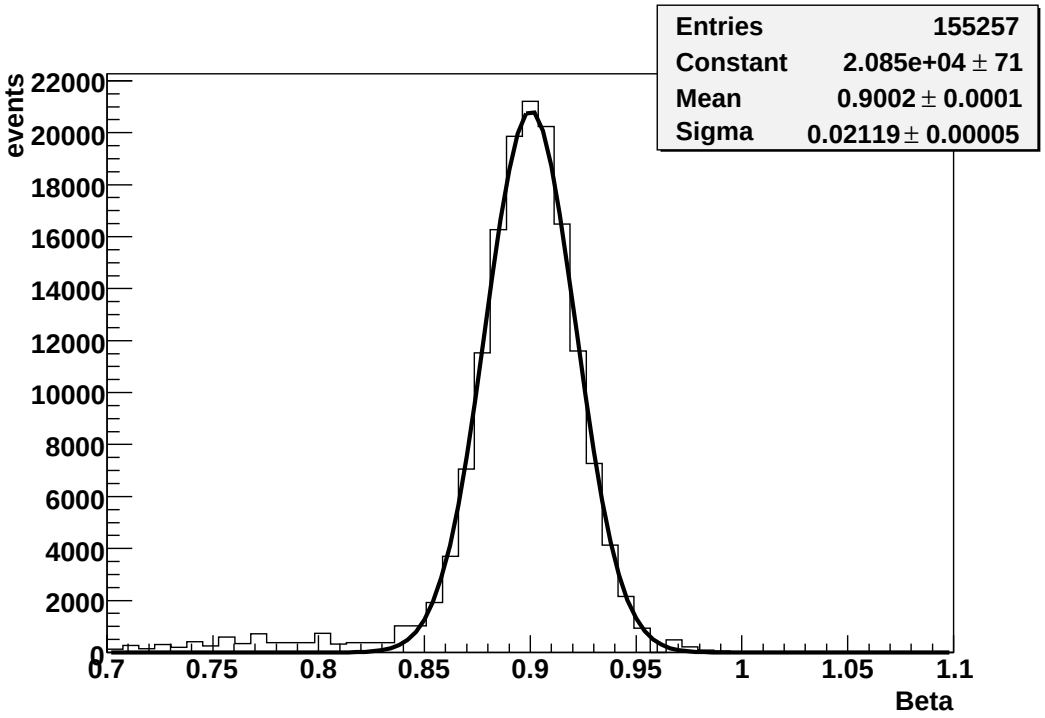

Fig. 6. Distribution of the velocity of particles β (in units of speed of light) measured between the planes S1 and S2 for a 1200 MeV/n ^{12}C beam.

Table 3
Resolution for time-of-flight and beta measurement

Ions	**Paddles**	**Theor. β**	**Measured Mean β**	Δt**(ps)**
^{12}C 1200 MeV/n	S1-S2	0.899	0.90±0.02	67
	S1-S3		0.902±0.019	62
^{12}C 200 MeV/n	S1-S2	0.568	0.568±0.009	61
	S1-S3		0.570±0.007	62
^{50}Cr 500 MeV/n	S1-S2	0.759	0.760±0.016	63
	S1-S3		0.760±0.015	68

By exposing the instrument to a monochromatic beam of particles with fixed kinetic energy (which is the same sample selected to evaluate K_1), the width of the distribution of the reconstructed β (an example is in figure 6) determines the time resolution on the measurements of *time of flight*, according to the simple relation $\Delta t = \Delta\beta\frac{L}{c\beta^2}$.

Table 3 summarizes the results of the measurements of time resolution of the TOF system with different beams and for different combinations of paddles.

For the determination of the particle velocity it is possible to use any combination of planes, like also planes S2 and S3, but being the distance between them of only 13 cm, the error $\Delta\beta$ will be much larger than for the other two combinations, therefore it was not used in our analysis.

The measured resolution is consistent with expectations and with tests in laboratory [11]. Since the actual β for a particle is derived from two paddles, we expect to the first order the simple propagation of errors:

$$\Delta t_{jk} = \sqrt{(\Delta t_{Sj})^2 + (\Delta t_{Sk})^2} \quad , \tag{4}$$

where Δt_{jk} is the resolution of the full TOF using DS, and Δt_{Sj} and Δt_{Sk} are the intrinsic errors of the paddles derived with the first method. In the most simple case this will just give a factor $\sqrt{2}$ if the paddles have the same intrinsic resolution. Results for C nuclei are in agreement with the results for the intrinsic resolution, as one can notice comparing values from tables 2 and 3, being $\Delta t_{Si} \simeq \Delta t/\sqrt{2}$ from the DS method.

5 Charge resolution for light nuclei

To study the charge resolution of TOF for light nuclei we tried to have a data sample widely spread out in energy so to simulate as well as possible the situation in flight. Therefore, the full available statistics for C beams has been considered, namely the ^{12}C beam at 1200 MeV/n, with and without target, and the sample at 200 MeV/n, with and without target, and recorded at angles of both 0° and 45°. First step of the analysis was the selection of the data sample to be analyzed. The initial data volume was reduced by an amount of 10-15% eliminating noisy events or small runs acquired in improper conditions.

The particle charge is determined by the energy deposits in any of the three TOF planes in conjunction with the velocity measurement from the TOF, that can be derived both by the top and the central and by the top and the bottom scintillators. The three scintillator layers enable three independent charge determinations, thus improving significantly the charge resolution.

The measurement of the energy released inside the scintillator by the passing particle is proportional to the mean charge deposited, Q, which can be measured by converting the ADC signal (in units of ADC channels) into charge (in units of pC) and correcting this value for the attenuation of light in the scintillator. By plotting this charge measurement versus the particle velocity we saw that points related to nuclei of different Z fall into different bands (figure 7); by fitting these bands it was possible to assign to every Z a mean value of charge deposit at the minimum of ionization.

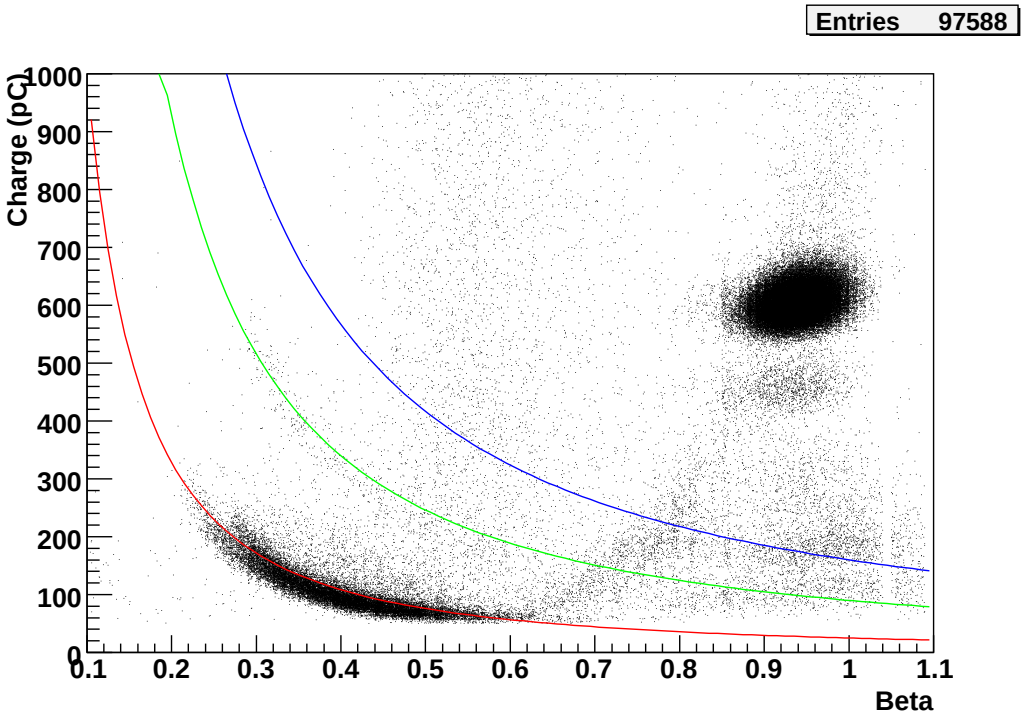

Fig. 7. The energy deposit in S2 as a function of the measured velocity β. The particles fall into charge bands. The 3 solid lines identify H, He, Li bands by means of phenomenological functions. The dark areas correspond to the particles with greater statistics in our sample. The three darkest areas are: Carbon ions of the beam at 1200 MeV/n (on the top-right), Boron ions (fragment) and low energy protons (recorded at angle of 45°). The β value used in this plot is not corrected for the *Time-Walk effect* and this explains the relatively big number of He and Li nuclei in the region with $\beta > 1$.

The results show that Q increases linearly with Z^2 in good approximation for S1 and S2, while for S3 a loss of linearity is observed (see figure 8). The behaviour can be justified by looking at the number of photoelectrons (PE) produced in each PMT, which is related to Q through the formula:

$$PE = \frac{Q}{e \cdot G} \quad , \tag{5}$$

where Q is the released charge, e is the charge of the electron and G is the gain of the PMT. The mean number of photoelectrons produced in S3 is greater than the one produced in S1 and S2 paddles, because S3 is thicker than S2 (more photons produced) and shorter than S1 (less attenuation). Apparently, hence, the charge released in S3 by the heavier ions covers a region of the dynamical range in which the system loses linearity.

To evaluate the contribution of this non-linearity of the PMT output, we

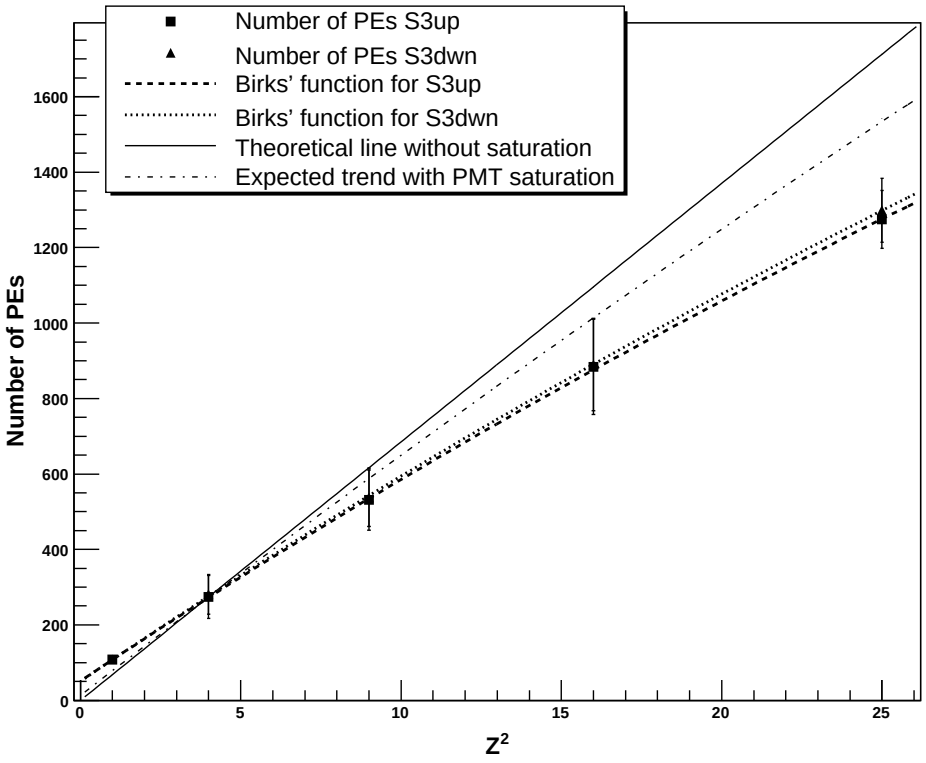

Fig. 8. Loss of linearity for S3 paddle versus Z^2 of the incident particle.

observe that, with our electronic base, the measured gain value of the R5900 PMT's is constant when the number of photoelectrons is lower than ~ 700; above this value the relation between the two quantities deviates gradually from linearity [1]. This deviation corresponds to a loss of gain of about 10% from ~ 700 to ~ 1100 PE (Be region) and about 15% from ~ 1000 to ~ 1500 PE (B region).

Figure 8 shows the comparison between the "ideal" behaviour of PE versus Z^2 (full line, obtained assuming that the gain is constant with Z) with the expected dependence taking into account the loss of gain of PMT's (dashed-dotted line) and the actual measurements of PE operated by the two PMTs associated to S3 which are affected by PMT saturation. Apparently the saturation of the PMTs is not sufficient to explain the loss of linearity. The

[1] Due to limitations on total weight and power budget for the TOF system, it was not possible to set-up a separate ADC acquisition chain exploiting the dynode signal of the PMT or use a different electronic base.

Table 4
CHARGE DISCRIMINATION FOR TOF

Nuclei	Z	**Paddle**	σ_Z
H	1	S2	0.08
		S3	0.07
He	2	S2	0.4
		S3	0.3
Li	3	S2	0.3
		S3	0.2
Be	4	S2	
		S3	0.3
B	5	S2	0.17
		S3	0.2
C	6	S2	0.15
		S3	0.17

experimental points were fitted by a 3-parameters function (dotted lines):

$$PE = p_0 + \frac{p_1 Z^2}{1 + p_2 Z^2} \quad . \tag{6}$$

By using this calibration function for a given PMT, it is possible to associate a value of Z to each particle by measuring the number of photoelectrons. The particle Z measured by a given paddle can be calculated as the mean between the two independent PMT measurements.

The plot of Z distribution for the paddles S2 and S3 is shown in figure 9, with Gaussian fits superposed on the data. The number of events relative to Protons and Carbons are divided by a factor 8 in order to make more visible the peaks for different values of Z.

Table 4 shows the charge resolutions (standard deviations of the Gaussian fits) obtained with the previous method for nuclei from H to C and for S2 and S3 paddles. The charge uncertainty is less than 0.1 for protons and 0.16 for C (in units of proton charge e). These results are extremely satisfactory for PAMELA TOF, since they are of the same order of magnitude of other space missions that measured nuclei and isotopes in the cosmic radiation, like the ISOMAX balloon-borne mission [12].

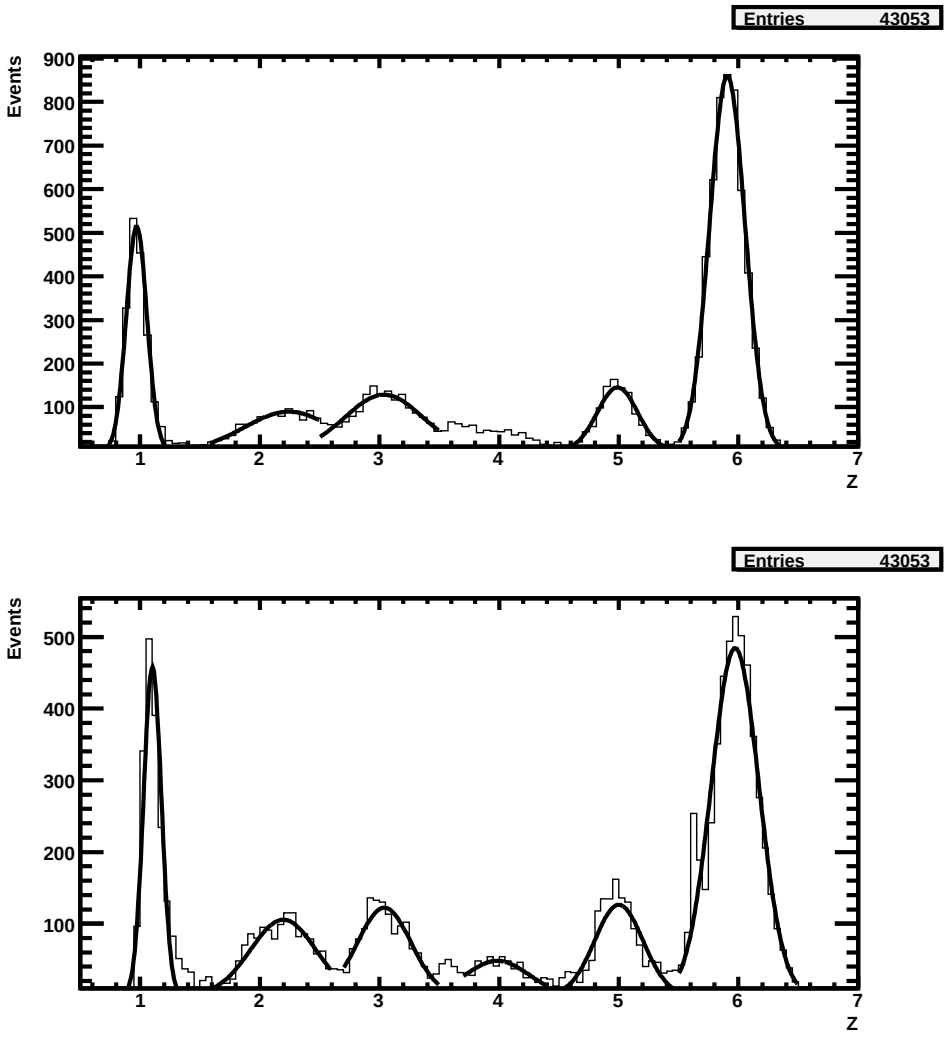

Fig. 9. Charge distribution obtained for particles with different beta and incident angle as measured by the TOF (top: paddle S2; bottom: paddle S3). The number of events for $Z = 1$ and $Z = 6$ are divided by a factor 8, in order to make more visible the peaks for different values of Z. Gaussian fits are superposed on the data.

Conclusion

This paper has shown the charge identification capabilities of PAMELA Time-Of-Flight system, as evaluated during a beam test. The test was performed at the GSI Laboratory in Darmstadt (Germany), in February 2006, with a technological copy of the PAMELA TOF and tracking system.

Monochromatic beams of Carbon and Chromium were used for the test, which lasted 4 days in a 24 hours/day cycle. By means of polyethylene and aluminum targets, and positioning the instrument at different angles with respect to the

beam axis, it was possible to study the charge resolution of the TOF for all light nuclei from Hydrogen to Carbon, and across a wide energy interval. Results show that the PAMELA Time-Of-Flight reaches very good performance in the identification of light-nuclei, thanks to the design and quality of the scintillating paddles.

Furthermore, beam test data were used to estimate the time resolution of the TOF, which resulted in agreement with laboratory tests.

Acknowledgments

We acknowledge the staff working at GSI, and especially dr. Dieter Schardt, for the excellent professionalism and friendly collaboration they offered us during our work in the laboratory. We would like also to thank the followings technicians of the INFN structure of Naples for their valuable contribution to the realization of the apparatus: P. Parascandolo, G. Passeggio, G. Pontoriere, E. Vanzanella.

References

[1] P. Picozza et al., Astropart. Phys, 2007, 27, p. 296.

[2] G. Barbarino et al., NIM A, 2008, 584, p. 319.

[3] G. Osteria et al., NIM A, 2004, 518, p. 161.

[4] G. Barbarino et al., Nuclear Physics B, 2003, 125, p. 298.

[5] S. Straulino et al., NIM A, 2004, 530, p. 168.

[6] S. Ricciarini et al., NIM A, 2007, 582, p. 892.

[7] W. Braunschweig et al., NIM 134, 1976, p. 261.

[8] M. Ambrosio et al., NIM A, 2002, 486, p. 663.

[9] D. Alvisi et al., NIM A, 1999, 437, Issues 2-3, p. 212.

[10] R. Carbone et al., NIM A, 2008, 588, Issues 1-2, p. 235.

[11] G. Osteria et al., NIM A, 2004, 535, p. 152.

[12] G. A. de Nolfo et al., The Astrophysical Journal, 2004, 611, p. 892.